Phys Chem Minerals (1996) 23: 1–10

ORIGINAL PAPER

J. Zhang · B. Li · W. Utsumi · R.C. Liebermann

In situ X-ray observations of the coesite-stishovite transition: reversed phase boundary and kinetics

Received April 3, 1995/Revised, accepted September 1, 1995

Abstract Using a DIA-type, cubic-anvil, high-pressure apparatus (SAM-85) in conjunction with *in situ* X-ray diffraction, we have investigated phase relations between coesite and stishovite up to 12 GPa and 1530 °C using synthetic powders of the two phases as the starting materials. The phase transition between coesite and stishovite was identified by observing the first appearance of a phase that did not already exist or by a change in the relative intensity of the two patterns. In most experiments, the diffraction patterns on samples were collected within 10 minutes after reaching a pressure and temperature condition. On this time scale, two phase boundaries associated with the coesite-stishovite transition have been determined: (1) for the stishovite-to-coesite transition, observations were made in the temperature range of 950–1530 °C, and (2) for the coesite-to-stishovite transition from 500 to 1300 °C. These observations reveal that there exists a critical temperature of about 1000 °C to constrain the coesite-stishovite equilibrium phase boundary. Above this temperature, both boundaries are linear, have positive dP/dT slopes, and lie within a pressure interval of 0.4 GPa. Below this temperature, the dP/dT slope for the stishovite-to-coesite phase boundary becomes significantly larger and that for the coesite-to-stishovite phase boundary changes from positive to negative. As a result, an equilibrium phase boundary can only be determined from the results above 1000 °C and is described by a linear equation P(GPa)=6.1(4)+0.0026(2)T(°C). This dP/dT slope is in good agreement with that of Zhang et al. (1993) but more than twice that of Yagi and Akimoto (1976). For the kinetics of the phase transition, preliminary rate data were obtained for the stishovite-to-coesite transition at 1160 and 1430 °C and are in agreement with the simple geometric transformation model of Avrami and Cahn.

Jianzhong Zhang · Baosheng Li · Wataru Utsumi
Robert C. Liebermann (✉)
Center for High Pressure Research and Department of Earth and Space Sciences, University at Stony Brook, Stony Brook, NY 11794, USA

Introduction

The phase transition between coesite and stishovite has been extensively used for pressure calibration at high temperature in multi-anvil experiments. Precise determination of the equilibrium coesite-stishovite phase boundary, along with the relevant P–V–T data, would provide important constraints on the thermochemical data such as heat capacity, enthalpy and entropy for coesite and stishovite. These data are, in turn, essential for a comprehensive understanding of the phase relations in the system $MgO-SiO_2$ (Saxena et al. 1993) but have not been well determined because of the back-transformation of high-pressure silica phases to an amorphous phase at high temperatures (Watanabe 1982) and contamination of the starting materials used in the calorimetric measurements (Akaogi and Navrotsky 1984).

Previous experimental efforts to study the coesite-stishovite transition have resulted in significant ambiguity in determinations of the phase boundary. In a general term, the dP/dT slopes of the phase boundary determined from quench experimental studies (e.g., Akimoto and Syono 1969; Suito 1977; Zhang et al. 1993) are significantly larger than those determined from the *in situ* X-ray measurements (Yagi and Akimoto 1976). Although the slopes obtained from the various quench studies are in reasonable agreement, the locations of the phase boundary differ in pressure by as much as 1 GPa at a given temperature (e.g., Akimoto 1972; Zhang et al. 1993).

The main reason for these inconsistencies lies in difficulties of performing true reversal experiments to observe the transition from coesite to stishovite. Such reversals have not been achieved in the *in situ* X-ray observations (Yagi and Akimoto 1976) and were difficult to demonstrate in the quench experiments (e.g., Akimoto and Syono 1969). In addition, each experimental technique has its own limitations. With the quenching technique, the uncertainty in pressure determination is a problem either because a room-temperature calibration

was used (Ostrovsky 1965; Akimoto and Syono 1969; Akimoto 1972) or the temperature range of the experimental study was beyond that of the pressure calibration (Zhang et al. 1993). With the previous *in situ* X-ray study (Yagi and Akimoto 1976), the transformation between coesite and stishovite is sluggish because most of the experiments were performed below 1000 °C. Additional complications arise because of the tendency for coesite to form metastably in the stability field of stishovite (e.g., Yagi and Akimoto 1976). Additional determinations using the *in situ* X-ray observations at temperatures above 1000 °C to reverse these phase transitions are therefore warranted to obtain an equilibrium phase boundary between coesite and stishovite.

In this paper, we report new data on the coesite-stishovite phase transition at temperatures of 500–1530 °C, obtained from the *in situ* X-ay diffraction observations. These data are used to constrain an equilibrium phase boundary and are compared with the previous studies. We also discuss kinetics of the transition from preliminary rate data obtained near the coesite-stishovite phase boundary.

Experimental methods

Experiments were performed using a DIA-type, cubic-anvil apparatus (SAM-85) designed for *in situ* X-ray diffraction studies at high pressure and temperature (Weidner et al. 1992, 1994). SAM-85 is a 250-ton uniaxial apparatus with an ability to reach conditions of 15 GPa and 1600 °C when using 4-mm sintered diamond anvils. An energy dispersive method was employed using white radiation from the superconducting wiggler magnet beamline at the National Synchrotron Light Source of Brookhaven National Laboratory. The incident X-ray beam was collimated to dimensions of 100×100 μm, and diffracted X-rays were recorded by the solid state Ge detector at a fixed angle of $2\theta=7.5°$. Data analysis was performed by a multichannel analyzer (MCA) in which 2048 channels were used. Typical times to collect each diffraction pattern were 150–200 s; in most experiments, the diffraction patterns on samples were collected within 10 min after reaching the chosen conditions of pressure and temperature.

Two types of cell assembly were used in this study and are shown in detail in Figs. 1 and 2. In both assemblies, a mixture of amorphous boron and epoxy resin was used as the pressure-transmitting medium. In the cylindrical-furnace assembly (Fig. 1), amorphous carbon was used as the heating material. Fine powder of stishovite or a mechanical mixture of stishovite+coesite were packed into one half of a boron nitride container of 1 mm diameter and 2 mm length; the other half contained NaCl as an internal pressure standard, mixed with powdered boron nitride to prevent recrystallization at high temperature. In the disk-furnace assembly, heating was provided by two graphite disks. The coesite sample and NaCl were placed within two separate boron epoxy sleeves of 0.8 mm diameter and 0.5 mm length. The coesite and stishovite samples used in this study were synthesized using the USSA-2000 (Liebermann and Wang 1992) at 1200 °C and pressures of 6 and 12 GPa, respectively, in a 14/8 mm cell assembly.

Temperature was measured by a W/Re 24%-W/Re 6% thermocouple that was at the center of the furnace and in direct contact with both the sample and NaCl layers (Figs. 1 and 2). Temperature variation over the entire sample length for the cylindrical furnace was of the order of 15 °C/mm at 1200 °C, and the radial temperature gradient was less than 10 °C/mm at these condition (Weidner et al. 1992, 1994). For the disk furnace, the temperature gradient is larger, approximately 40 °C/mm at 1000 °C (Utsumi et al. 1994).

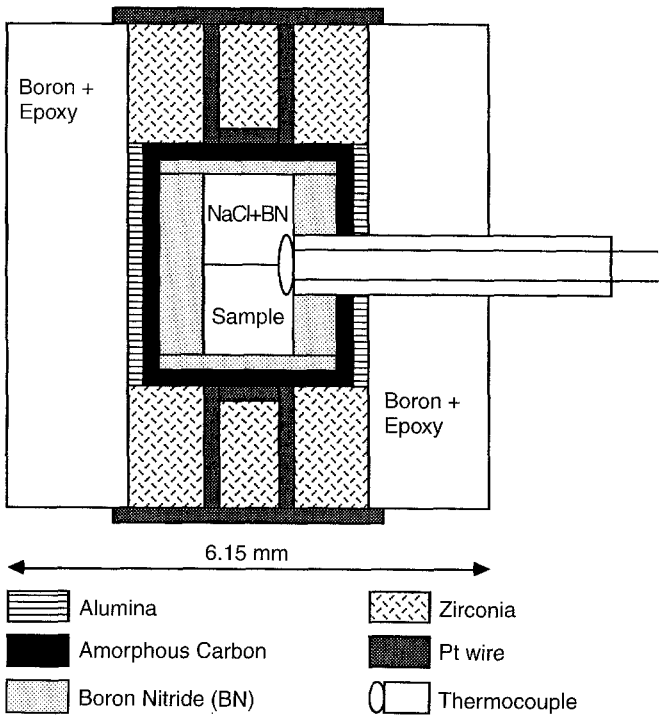

Fig. 1 Cell assembly of the cylindrical furnace (modified from Weidner et al. 1992)

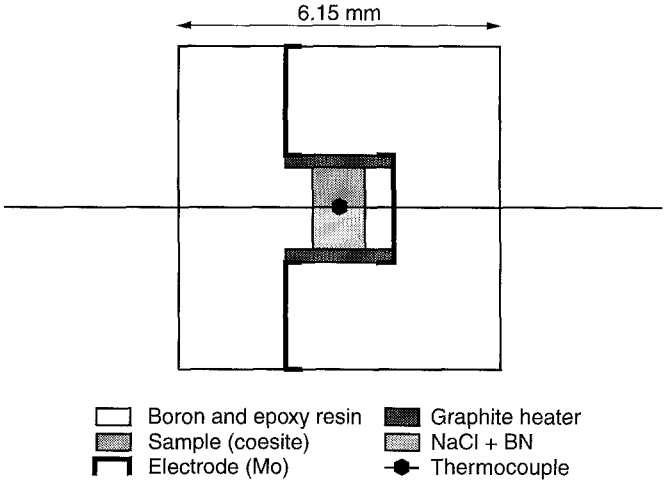

Fig. 2 Cell assembly of the disk-type furnace (from Utsumi et al. 1994)

Diffraction patterns, however, were usually obtained from both the sample and the NaCl pressure standard in close proximity to the thermocouple junction, and errors in temperature measurements of the study were thus estimated to be ±10 °C. No correction for the effect of pressure on thermocouple emf was applied.

Pressure values were calculated from Decker's equation of state for NaCl (Decker 1971) using lattice parameters determined from X-ray diffraction profiles at each experimental condition; no correction was made for the deviatoric stress at low temperatures. Four diffraction lines, (200), (220), (222), and (420), were usually used for determination of the pressure. The uncertainty in pressure determination is mainly attributed to the inconsistency among the different diffraction lines and is generally less than 0.2 GPa in the pressure range of the study. No evidence of a vertical or radial

pressure gradient was indicated at room temperature in the sample chamber (Weidner et al. 1992).

In each experiment, pressure was applied first at room temperature, and the temperature was then raised to the desired value at constant ram load. The subsequent experimental P–T path depended on whether the transition was observed and the direction of the transition (i.e., coesite to stishovite or stishovite to coesite); typical experimental P–T paths are shown in Figs. 3 and 4. For both assemblies used in this study, the sample pressure always decreases in the first heating cycle because of the flow of pyrophillite gaskets and the decrease of the deviatoric stress with increasing temperature (Weidner et al. 1992, 1994); this made it convenient to observe the phase transition from stishovite to coesite by either directly crossing the phase boundary with continuous heating (paths 1 and 2 in Fig. 3) or by decreasing pressure at a constant temperature (path 3 in Fig. 3) until coesite began to form.

To observe the transition from coesite to stishovite, it was necessary to increase pressure at high temperature because of the positive dP/dT slope of the phase boundary. These experiments were performed using the following procedures. The temperature was first increased to a certain value (usually up to 800 °C) at constant ram load in the field of coesite and then quenched (path 1 in Figs. 4a and 4b). Along this path, the pressure decreased significantly due to relaxation of the deviatoric stress during heating and loss of thermal pressure during quenching (Weidner et al. 1992, 1994). Pressure was then increased at room temperature to a value that depended on the experimental destination. During the second heating cycle, the pressure was observed to increase up to the peak temperature (800 °C) of the previous heating cycle because of the recovery of the thermal pressure and then started decreasing with increasing temperature (path 2 in Fig. 4a and path 3 in Fig. 4b). As a result of the P–T characteristics of each cell, it was necessary to adopt other procedures to ensure the observation of the phase transitions at specific pressures, including: (a) compression at high temperature (path 2 in Fig. 4a); and (b) heating very close to the phase boundary and then decompressing at high temperature (path 4 in Fig. 4b).

The cylindrical-furnace assembly (Fig. 1) was used for observing the transition from stishovite to coesite and the disk-furnace assembly (Fig. 2) for the transition from coesite to stishovite. The major difference between these two assemblies is that the pressure loss during the first heating cycle using the cylindrical-furnace assembly is larger than that using the disk-furnace assembly (Figs. 3 and 4); this is primarily because the cylindrical-furnace assembly has a large sample size and uses a boron nitride container which is soft and may experience phase transition from hexagonal to wurtzite-type structure, accompanied by a large volume reduction, at pressure above 10 GPa and high temperature (Shimomura et al. 1994).

Throughout this work, two diffraction lines of coesite: (130+111), (040+200), and one line of stishovite: (110), were

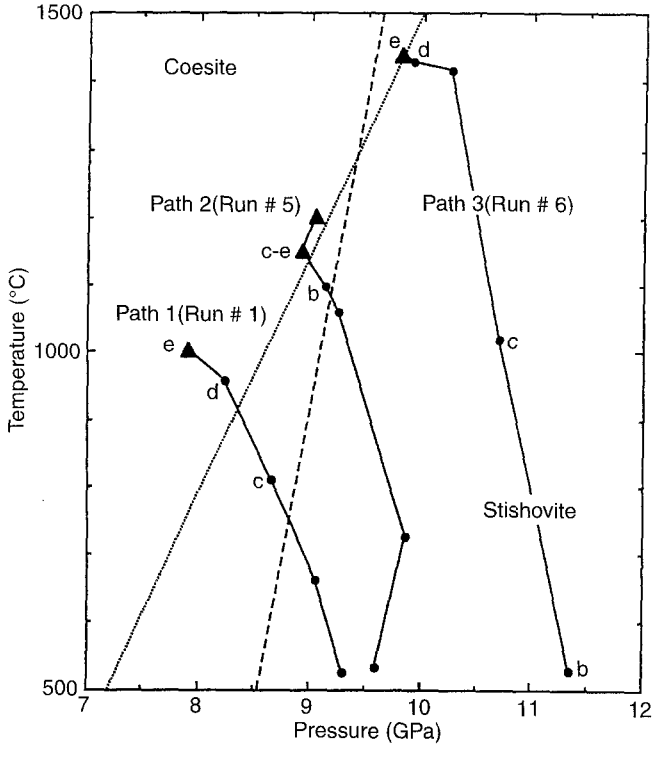

Fig. 3 Typical experimental P–T paths to observe the stishovite-to-coesite transition. The *dash* and *dotted lines* are the coesite-stishovite phase boundary determined by Yagi and Akimoto (1976) and Zhang et al. (1993), respectively. *Solid circles* are the experimental data points, and *solid triangles* represent pressure and temperature at which the transition from stishovite to coesite was observed. *Small letters* of a, b, c, etc. correspond to the X-ray spectra shown in Figs. 5, 6 and 7

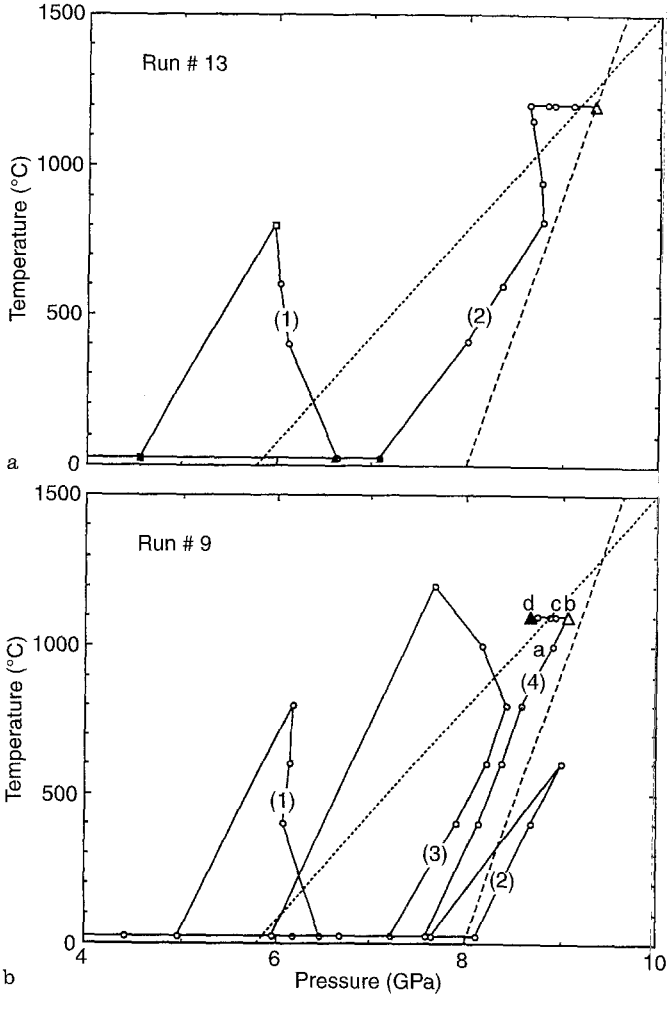

Fig. 4a, b Typical experimental P–T paths to observe the coesite-to-stishovite transition. **a** Compression at 1200 °C to observe the phase transition. **b** Reversal of the coesite-stishovite transition at 1100 °C in a single experiment. *Open circles* are the experimental data points; *open* and *solid triangles* represent pressures and temperatures at which the coesite-to-stishovite and stishovite-to-coesite transitions were observed, respectively. *Small letters* of a, b, c, d in Fig. 4b represent the pressure and temperature conditions of the X-ray spectra shown in Fig. 8

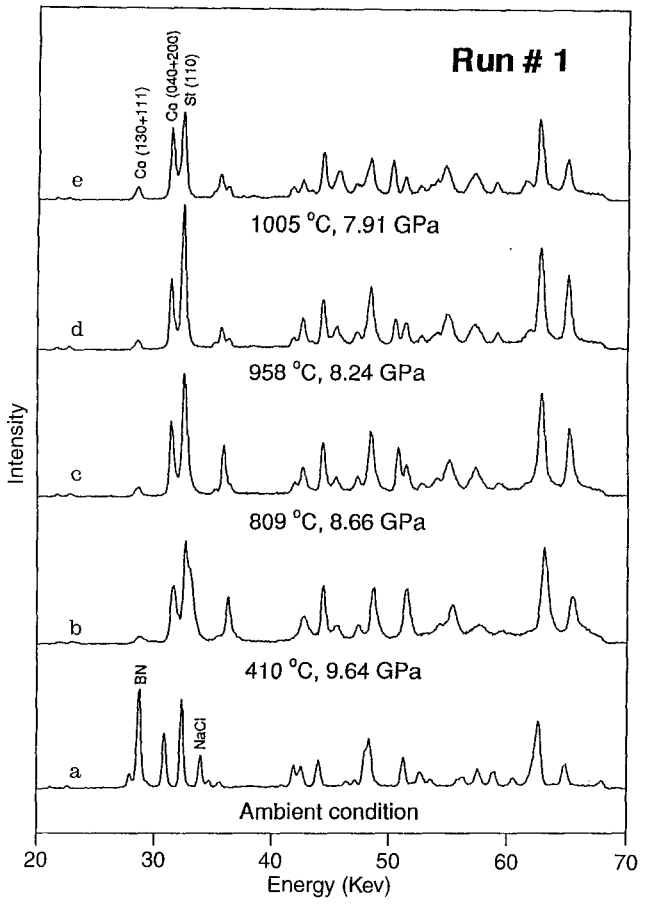

Fig. 5 Selected X-ray spectra as a function of temperature for Run # 1 (see P–T path in Fig. 3). It is seen that the relative intensity of coesite (both 130+111 and 040+200 diffraction peaks) becomes significantly stronger when temperature increased from 958 °C (*d*) to 1005 °C (*e*), indicating growth of coesite at the expense of stishovite

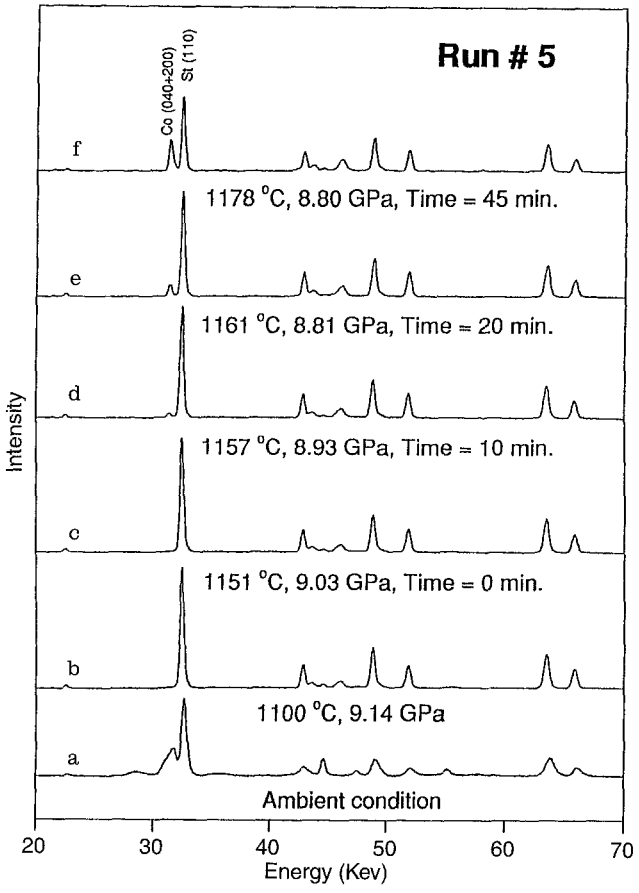

Fig. 6 Selected X-ray spectra for Run # 5 showing the first appearance and growth of coesite as a function of time at the constant temperature and pressure. Coesite started forming (*d*) after staying 10 min at 1151 °C and 9.03 GPa (*c*); (*d*) to (*f*): the relative intensity of coesite increased with time at constant P and T (Note: the temperature slightly increased with time without change of power to furnace)

used for phase identification. For a mixture of coesite and stishovite as the starting material the phase transition was identified by observing a significant change in the relative intensity between two phases (e.g., spectrum e in Figs. 5 and 8). For a pure phase of coesite or stishovite in the sample, we observed the first appearance of a phase that did not already exist (e.g., spectrum d in Fig. 6 and spectrum e in Fig. 7). The phase identification were made by moving the X-ray beam to a fixed position of the sample chamber which usually did not change during heating.

Results and discussion

Experimental observations

Experimental results were obtained in the pressure and temperature ranges of P=7.5–11.5 GPa and T=500–1530 °C (see Table 1). For a mixture of coesite and stishovite as the starting material, it was always observed that coesite in the mixture would begin to transform to stishovite when the temperature exceeded 500 °C for pressures higher than 9.5 GPa (spectra b and c in Fig. 7). With further heating, coesite disappeared rapidly and stishovite usually remained as a single phase at temperatures above 750 °C (see spectra b and c in Fig. 6 and spectra c and d in Fig. 7). This indicates that in this pressure range it would make no difference for the experimental results whether stishovite or a mixture of the SiO_2 phases were used as the starting material. At or near the experimental conditions of the transition, both the coesite-to-stishovite and the stishovite-to-coesite transitions were observed to occur either by increasing temperature of 50–100 °C (see spectra d to e in Fig. 5 and spectra b to c in Fig. 8) or by maintaining constant P–T conditions for a period of 10–15 min (see spectra c and d in Fig. 6).

The phase transition between coesite and stishovite has been fully reversed in a single experiment in this study (see P–T path for Run # 9 in Fig. 4b). In this experiment, coesite was used as the starting material, and special attention was paid to follow P–T paths which preserved the coesite and prevented transition to stishovite (see paths 1, 2, 3 and 4 below 1000 °C). The first appearance of stishovite was observed at 9.06 GPa and 1100 °C (spectrum c in Fig. 8), and was confirmed in

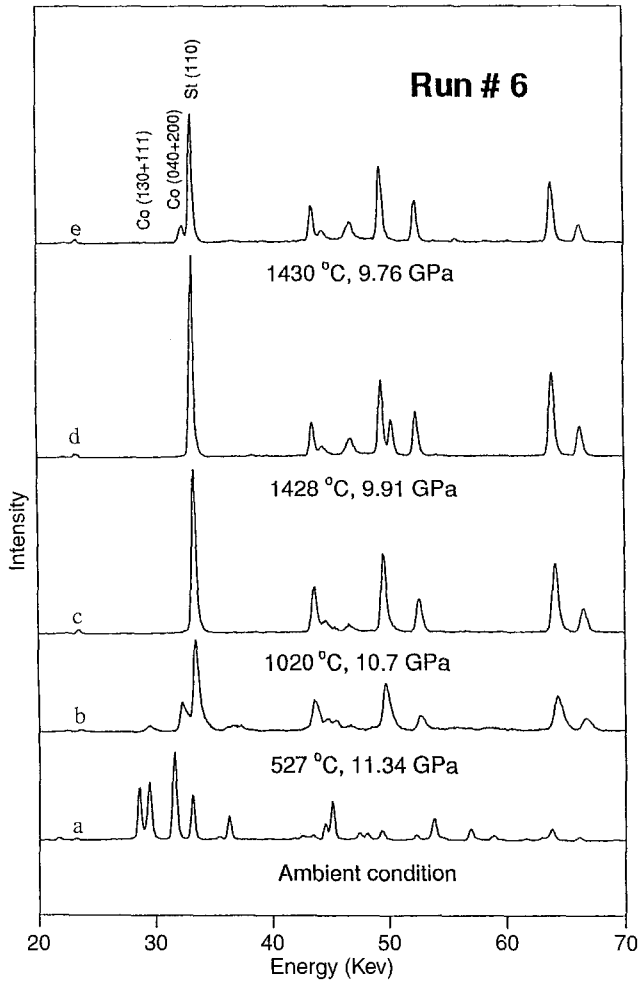

Fig. 7 Selected X-ray spectra for Run # 6. (*b*) The relative intensity of coesite decreased dramatically at 527 °C and 11.34 GPa compared to that of the starting material (*a*), indicating the transition from coesite to stishovite. (*e*) Coesite started forming again at 1430 °C and 9.76 GPa; it is important to mention that no transition was observed after staying at 1428 °C and 9.91 GPa (*d*) for a period of 10 min

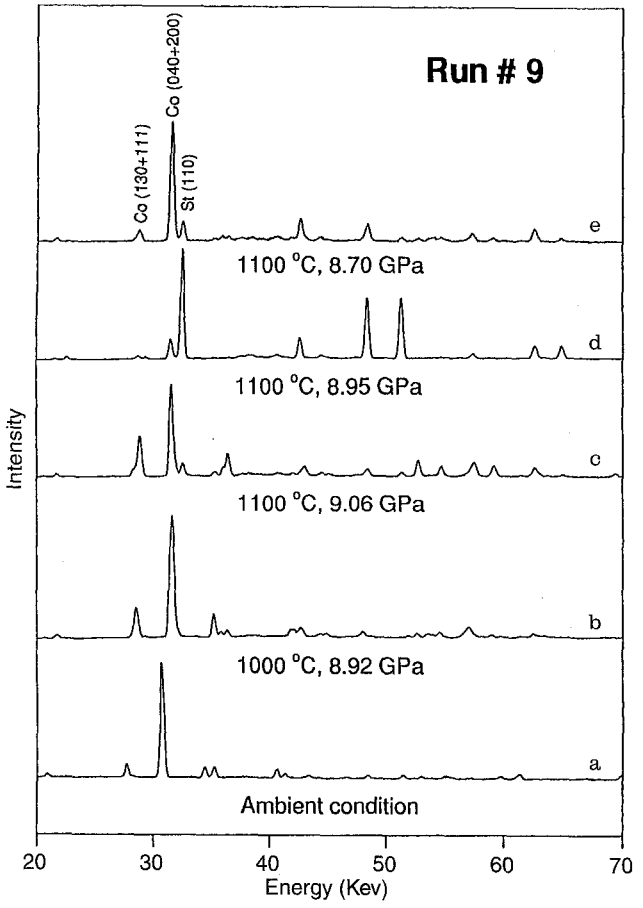

Fig. 8 Selected X-ray spectra for Run # 9 showing the reversal of the coesite-stishovite transition in a single experiment (see Fig. 4 b for the P–T paths). (*b*) No transition was observed at 1000 °C and 8.92 GPa for a period of 10 min; (*c*) stishovite started forming from coesite at 1100 °C and 9.06 GPa; (*d*) collected 30 min after (*c*) without changing the P–T condition, the relative intensity of stishovite became stronger than that of coesite throughout the sample chamber; (*e*) ratio of the relative intensity between coesite and stishovite reversed compared to that of (*d*) after the slow decompression at 1100 °C for a period of about 45 min

the other parts of the sample. After staying at this condition for about 30 minutes to make the relative intensity of stishovite stronger than that of coesite throughout the sample chamber (spectrum d in Fig. 8), pressure was then reduced gradually at the constant temperature. At 8.7 GPa, the ratio of the relative intensity between coesite and stishovite reversed (spectrum e in Fig. 8) compared to that prior to the decompression (spectrum d in Fig. 8), indicating the growth of coesite at the expense of stishovite. As a result, we have bracketed the coesite-stishovite transition within 0.4 GPa at the temperature of 1100 °C.

The coesite-to-stishovite transition was also observed at about 1200 °C and 1300 °C, in Run # 13, although reversal of the transition was not attained in the same experiments because of subsequent thermocouple failure and strong recrystallization of NaCl pressure standard and the samples after a long period of time at high temperatures. From comparison with the observations for the stishovite-to-coesite transition at similar temperatures (see Table 1 for Runs # 5 and 12), however, we find that the coesite-stishovite transition at 1200–1300 °C is also bracketed in a pressure interval of less than 0.4 GPa, consistent with the experimental results obtained at 1100 °C in Run # 9.

Another critical experiment in this *in situ* study is Run # 6 (Table 1, Figs. 3 and 7). As the temperature was increased from 527 to 1020 °C, the coesite-stishovite mixture (Fig. 7 b) was totally converted to stishovite (Fig. 7 c); no change was observed on further heating to 1415 °C. At fixed furnace power and constant temperature, the pressure was decreased gradually from 10.25 to 9.91 GPa with no sign of coesite growth (Fig. 7 d), even during a period of 10 min at 9.91 GPa. However, as the pressure was lowered by less than 0.2 GPa over a period of 9 minutes, coesite began to appear (Fig. 7 e). These observations indicate that the transition from stishovite to coesite was well determined at these P–T conditions.

Table 1 Experimental results for the observed coesite-stishovite transition

Run No.	Starting material	Cell assembly	Pressure GPa	Temperature °C	Type of the transition
COST 1	Co+St	cylindrical	7.91	1005[1a]	St to Co
COST 3	Co+St	cylindrical	7.99	985	St to Co
COST 4	Co+St	cylindrical	8.36	1024	St to Co
			8.47	1034	St to Co
			8.62	1234	St to Co
COST 5	Co+St	cylindrical	9.70	608	Co to St
			9.81	726	Co to St
			8.93	1157	St to Co
			8.79	1166	St to Co
			9.04	1203	St to Co
COST 6	Co+St	cylindrical	11.36	527	Co to St
			9.76	1430[1b]	St to Co
COST 8	Co	cylindrical	10.32	598	Co to St
			9.35	700	Co to St
COST 9	Co	disk	9.06	1100	Co to St
			8.70	1100	St to Co
COST 10	St	cylindrical	8.17	1002	St to Co
COST 12	St	cylindrical	9.30	1300[1c]	St to Co
COST 13	Co	disk	9.32	1205	Co to St
			9.71	1211	Co to St
			9.63	1299	Co to St
COST 14	St	cylindrical	10.04	1530	St to Co
COST 15	St	cylindrical	7.71	985	St to Co
			7.74	960	St to Co

[1a] thermocouple failed 850°C; [1b] thermocouple failed the temperature given in the table; [1c] thermocouple failed at 1050°C (Co=coesite; St=stishovite). In these runs, temperatures were estimated from the power-temperature relations

At 1430 °C in Run # 6 and at 1530 °C in Run # 14, the NaCl pressure standard started melting, and the diffraction peaks became weak compared to those collected at other conditions. However, three diffraction peaks of NaCl were still available for determination of pressures at the P–T conditions of both experiments. More importantly, as shown in Table 2, the cell parameters calculated from each individual peak are in good agreement, indicating that the pressures at these temperatures are well determined.

Table 2 Unit cell parameters of NaCl and the determined pressures

hkl	d-space, Å	Cell volume, Å^3	Pressure, GPa
T=1430°C, Run # 6			
(111)	3.0854	152.63	9.82
(200)	2.6731	152.80	9.77
(222)	1.5440	153.01	9.70
Average pressure: P=9.76 GPa			
T=1530°C, Run # 14			
(111)	3.0842	152.46	10.17
(200)	2.6744	153.04	9.99
(220)	1.8916	153.13	9.96
Average pressure: P=10.04 GPa			

After the transition were observed, the relative intensities between coesite and stishovite changed with time at constant pressure and temperature (e.g., Fig. 6 d–f). For the transition from stishovite to coesite, it is clear that coesite grows at the expense of stishovite with time (Fig. 9 a). The transformation kinetics are in agreement with the rate equation using well-known Avrami relation for the transformed mass or volume fraction (Fig. 9 b), indicating a transition characterized by a nucleation and growth mechanism (Christian 1975).

Following the Avrami relation, $X=1-\exp(-Kt^n)$, the linear regression of the data in Fig. 9 b gives values of $K=1.2\times10^{-7}\,s^{-n}$ for the rate constant and $n=1.9$ at 1160 °C and $K=5.1\times10^{-7}\,s^{-n}$ and $n=2.0$ at 1430 °C. From these values, two preliminary conclusions are drawn for the kinetics of the transition from stishovite to coesite. Firstly, the rate constant K increases with increasing temperature at constant pressure (see Fig. 9 a). Secondly, the values of the exponent n at 1160 °C and 1430 °C are less than 2. According to the theory of Cahn (1956), this suggests that the stishovite-to-coesite transformation at these conditions is characterized mainly by the growth stage of a grain-boundary nucleated solid-solid transformation.

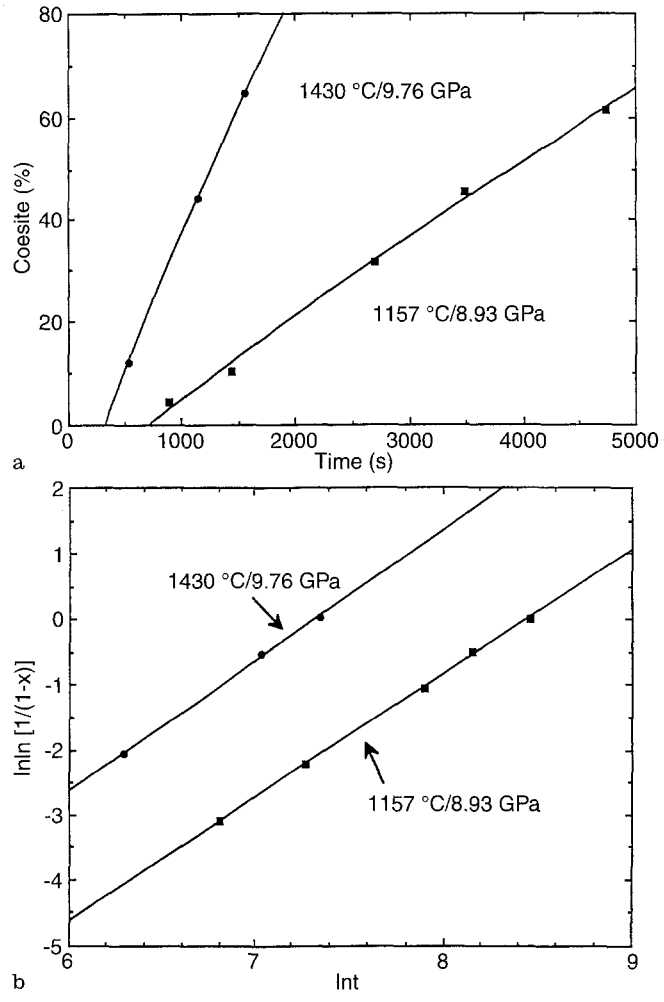

Fig. 9 **a** Volume fractions of coesite transformed from stishovite (X_{co}) as a function of time (t). $X_{co}=I_{co\,(040+200)}/[I_{co\,(040+200)}+I_{st(110)}]$, where $I_{co\,(040+200)}$ and $I_{st(110)}$ are the most intense diffraction peaks for coesite and stishovite, respectively. **b** Plot of ln ln $[1/(1-X_{co})]$ versus ln t. Excellent linear relation between these data suggests that the transformation kinetics for the stishovite-to-coesite transition can be described by the Avrami rate equation: $X=1-\exp(-Kt^n)$, where X is the isothermal or isobaric data of the transformed volume fractions, which can be obtained from Fig. 9 a, K the rate constant, and n an exponent that characterizes the transformation process

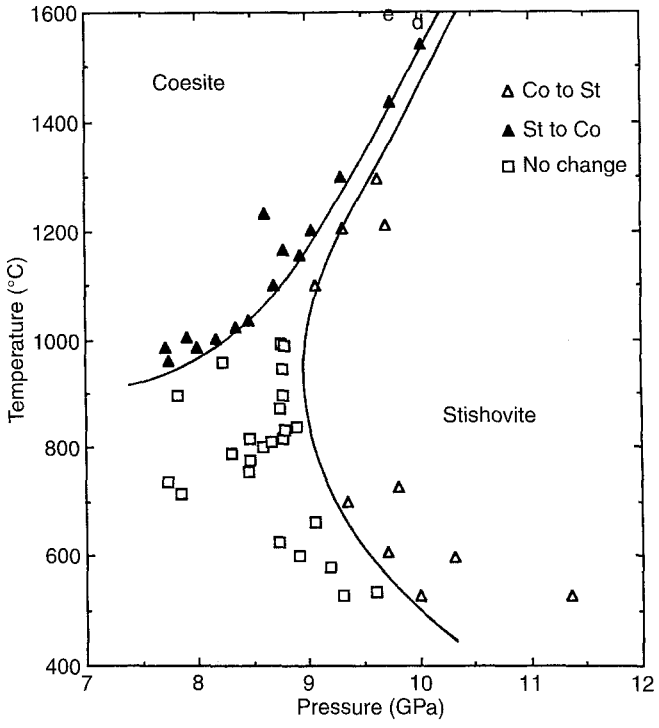

Fig. 10 Experimental results of the present *in situ* experiments (see also Table 1). *Open triangles* are for the transition from coesite to stishovite and *solid triangles* for the transition from stishovite to coesite. *Squares* indicate the pressure and temperature conditions at which no transition was observed on the time scale of the experiments. The two *solid curves* represent the kinetic phase boundaries for the coesite-to-stishovite and the reversed transitions

Equilibrium versus kinetic phase boundaries

The experimental results for the coesite-stishovite transition are summarized in Fig. 10. In this P–T space, the results are internally consistent for all of the 12 experimental runs performed using different starting materials and cell assemblies (see details in Table 1). Two kinetic phase boundaries that are associated with the stishovite-to-coesite and the coesite-to-stishovite transitions have been determined in the temperature ranges of 950–1530 °C and 500–1300 °C, respectively; these provide the lower and upper bounds in pressure at a given temperature for the coesite-stishovite transition.

An inspection of Fig. 10 demonstrates that there exists a critical temperature of about 1000 °C for determining the equilibrium phase boundary. Above this temperature, the two kinetic phase boundaries are linear and have positive dP/dT slopes. They are bracketed within a pressure interval of 0.4 GPa and seem to converge with increasing temperature. From these high temperature data, an equilibrium phase boundary for the coesite-stishovite transition can be determined and is given by

$$P(\text{GPa})=6.1(4)+0.0026(2)\,T(^\circ\text{C}) \quad (1)$$

where the uncertainties are calculated from the misfit of the experimental data. The errors in determinations of pressure and temperature are not included in the fitting procedure but are much smaller than those given above.

Below 1100 °C, the dP/dT slope for the stishovite-to-coesite phase boundary becomes significantly larger and that for the coesite-to-stishovite phase boundary changes from positive to negative. As a result, the two phase boundaries diverge rather rapidly with decreasing temperatures. Between the two boundaries, there is a "region of indifference" in which no transition was observed, irrespective of which starting material (coesite or a mixture of coesite and stishovite) was used in the experiments. From these results, we conclude that the equilibrium coesite-stishovite transition cannot be determined at temperatures below 1000 °C on the time scale of the present experiments.

By comparing the Eq. (1) with the two kinetic boundaries of Fig. 10, it is clear that the phase transition cannot start immediately at the equilibrium phase boundary in the entire temperature range of the study. The metastable overshoot (ΔP) is required to provide a sufficiently large energy driving force (ΔG_f) and to overcome a nucleation barrier for the transitions to occur following the relation $\Delta G_f = \Delta V \Delta P$, where ΔV is the volume change upon the transition. Qualitatively, this overshoot is very small, less than 0.2 GPa between 1100–1530 °C, but increases rapidly with decreasing temperature, indicating that a substantial nucleation barrier exists for the coesite-stishovite transition at low temperatures. In view of the fact that the coesite-to-stishovite transition was observed at temperatures above 500 °C while the stishovite-to-coesite transition can not be observed below 900 °C in the experimental pressure range (Fig. 10), we conclude that the nucleation processes are asymmetric and that the nucleation barrier for the forward transition (from coesite to stishovite) is smaller than that for the backward transition (from stishovite to coesite). The sluggishness of the reaction kinetics for the coesite-stishovite transition below 1000 °C may be associated with a large activation energy at low temperatures to change the Si^{4+} coordination in coesite and stishovite from 4-fold and 6-fold.

Comparison with previous studies

Comparison of the present study with the previous determinations is shown in Fig. 11 (see also Table 3). For the equilibrium coesite-stishovite phase boundary, the dP/dT slope of this work is more than twice that determined by Yagi and Akimoto (1976), but in good agreement with those of the studies determined from quench experiments (Akimoto and Syono 1969; Akimoto 1972; Suito 1977; Zhang et al. 1993). With regard to the discrepancies between the two *in situ* X-ray diffraction studies, we consider the following issues.

The primary difference is that no true reversal experiments (in the sense that the forward and backward transitions are determined at fixed temperature) have been achieved from the Yagi and Akimoto study, although they emphasized that the coesite formed from stishovite at 1050 °C and 1100 °C in their study can be regarded as the transition of this kind. By examining the original data of Yagi and Akimoto, we note that at high temperatures of 1050 °C and 1100 °C where the rates of the transition are expected to be much faster, their data are in agreement with those of this study for the stishovite-to-coesite transition. However, these data appear to be inconsistent with their fitted phase boundary (P=8.0+0.0011 T) and suggest a much larger dP/dT slope (Fig. 11). Such a discrepancy can be easily interpreted because these data can be only considered as the lower bound in pressure for the equilibrium coesite-stishovite boundary, particularly in this temperature range where a large metastable overshoot is required with decreasing temperature.

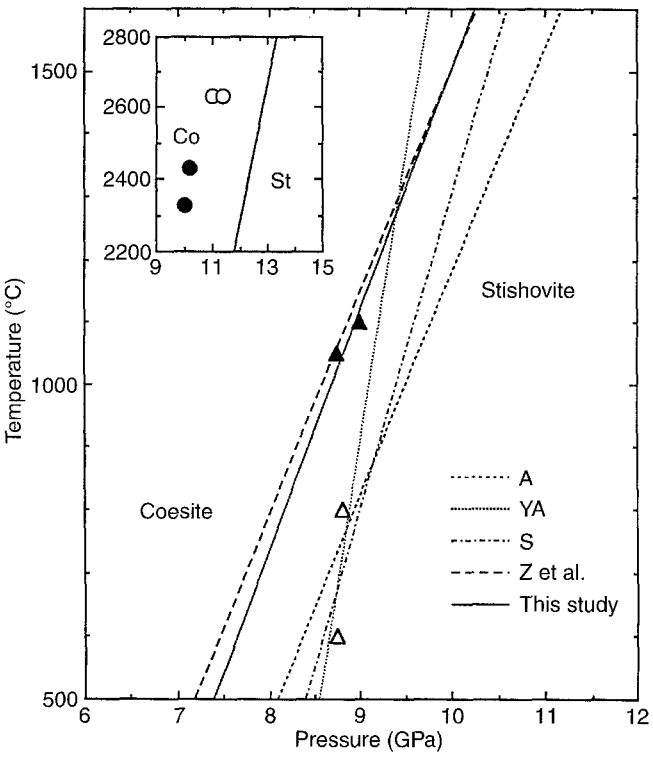

Fig. 11 Comparison of the coesite-stishovite phase boundary of this study with those of the previous studies (see also Table 3). Crucial data of Yagi and Akimoto (1976) from *in situ* X-ray measurements and Serghiou et al. (1995) using a laser-heated DAC are shown, respectively, as *triangles* and *circles*: *solid symbols* for the transition from stishovite to coesite and *open symbols* for the transition from coesite to stishovite. A: Akimoto 1972; YA: Yagi and Akimoto 1976; S: Suito 1977; Z et al.: Zhang et al. 1993. The phase boundary of Serghiou et al. (1995) is not plotted here because it is almost identical to the one of Yagi and Akimoto (1976)

Table 3 Slope dP/dT of coesite-stishovite phase boundary

Reference	dP/dT (GPa/°C)	Type of study
Akimoto & Syono (1969)	0.0028	Quench
Yagi & Akimoto (1976)	0.0011	*In situ* X-ray
Suito (1977)	0.0020	Quench
Zhang et al. (1993)	0.0028	Quench
Serghiou et al. (1995)	0.0010	Laser-heated DAC
This study	0.0026	*In situ* X-ray

The transition from coesite to stishovite was indeed observed in the Yagi and Akimoto study but at temperatures of 600 and 800 °C using amorphous silica as the starting material (Fig. 11). At these relatively low temperatures, our results show that kinetics of the transition are very sluggish, which makes it impossible to observe the transitions between coesite and stishovite on the time scale of the experiments. We have no definite explanation why the transition was observed at a temperature as low as 600 °C in their experiments, but the metastable coesite, formed below 500 °C in the stability field of stishovite when using amorphous silica as the starting material, may be energetically less stable than the syn-

thetic coesite used in this study. Consequently, these observations can only provide a upper bound in pressure for the equilibrium phase boundary. An inspection of Fig. 11 demonstrates that the critical data of Yagi and Akimoto (1976) are compatible with slopes of dP/dT as low as 0.001 GPa/°C and as high as 0.004 GPa/°C.

It should not be surprising that the dP/dT slope of this work is in agreement with those of the quench studies (Table 3). Although the pressure determinations using the quench method are not as accurate as using the *in situ* X-ray technique, the slope of a phase boundary can be determined with a reasonably good accuracy if the pressure calibration is internally consistent. More importantly, the quench experiments can be conducted at very high temperatures (e.g., 2000–2800 °C in the study of Zhang et al. 1993) or for a long time duration (e.g., a few hours at a constant P and T in the experiments of Akimoto and Syono 1969), which minimize the effect of the kinetics on the phase transition.

Concluding remarks

The present *in situ* X-ray observations between 1100 and 1530 °C yield an equilibrium phase boundary for the coesite-stishovite transition, and can be used with confidence for the pressure calibration at high temperature in the 9–11 GPa range. It is suggested that such calibration experiments be performed at temperatures above 1000 °C with the following calibration fixed points: 8.7 GPa at 1000 °C, 10.0 GPa at 1500 °C and 11.3 GPa at 2000 °C. These values differ by $\Delta P = -0.5$ GPa at 1000 °C and +1.0 GPa at 2000 °C from those implied by the Yagi and Akimoto (1976) data which have been widely used in the high-pressure experimental studies.

By assuming a linear extrapolation of the phase boundary of this work to the melting temperatures of coesite and stishovite determined by Zhang et al. (1993), the coesite-stishovite-liquid triple point is located at 13.3 GPa and 2800 °C, which is very similar to the one (13.7 GPa at 2800 °C) reported in the Zhang et al. study. Using this triple point and the new melting data of Shen and Lazor (1995) for stishovite at high pressures, a revised phase diagram for SiO_2 is obtained and shown in Fig. 12.

Since an equilibrium phase boundary has been obtained from this work, it provides a critical cross-check for the thermodynamic data of coesite and stishovite obtained from other independent studies (e.g., Akaogi and Navrotsky 1984; Fei et al. 1990). It is emphasized that precise determination of these data is crucial because stishovite is also an important constituent in the phase relations of $MgSiO_3$ where it is involved in several reactions of interest in geochemistry and geophysics. Note that since the present work shows that the dP/dT slope of the coesite-stishovite boundary is more than twice that determined by Yagi and Akimoto (1976), the conclusion drawn by Zhang et al. (1993) remains applicable for this study: i.e., a significant increase in the entropy change

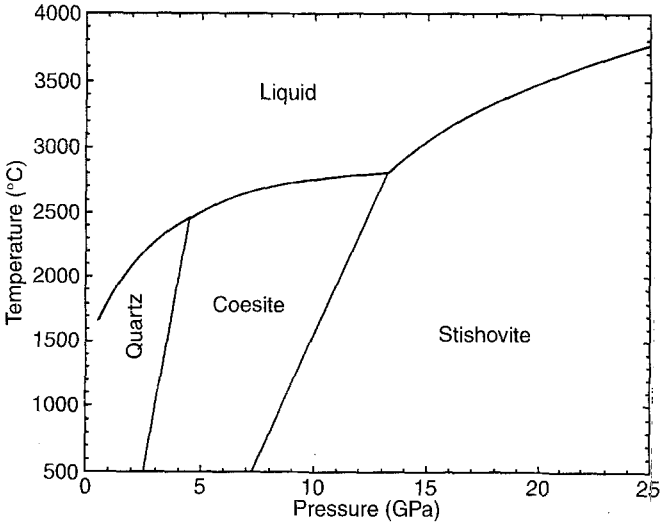

Fig. 12 Phase diagram for SiO_2. Melting data for quartz are from Jackson (1976) and Kanzaki (1991), for coesite from Kanzaki (1991) and Zhang et al. (1993), and for stishovite from Zhang et al. (1993) and Shen and Lazor (1995). Subsolidus data for quartz-coesite transition are from Bohlen and Boettcher (1982) and for the coesite-stishovite transition from this study and Zhang et al. (1993)

of the transformation, compared with the value ($\Delta S = -4.2 \pm 1.7\ J K^{-1} mol^{-1}$) of Akaogi and Navrotsky (1984), is required to be consistent with the most recent experimental determinations.

After we completed and reported our new *in situ* experimental data (Zhang et al. 1992, 1994), Akaogi et al. (1995) and Liu et al. (1996) have re-determined the enthalpy of both coesite and stishovite and re-calculated the entropy change across the transition. The ΔS^0_{298} values of the two independent studies are consistent but more than three times larger in magnitude than those of Akaogi and Navrotsky (1984). Thermodynamic calculations from these new measurements and other relevant data by both sets of authors indicate a coesite-stishovite phase boundary that is in excellent agreement with the experimental results of this study and those of Zhang et al. (1993).

After this paper was submitted for publication, a paper by Serghiou et al. (1995) has been published. They studied the coesite-stishovite transition in a CO_2-laser heated diamond-anvil cell and reported a phase boundary that is described by the equation P(GPa)=8.0+0.001 T(°C), thus in disagreement with the present result. We note that the slope dP/dT of the phase boundary cannot be solely determined from the experimental data of Serghiou et al. (1995); it is instead obtained by a combination of their observations at 2330–2630 °C (see Fig. 11) and those of Yagi and Akimoto (1976) at temperatures below 1100 °C. In this approach, however, uncertainties may arise from the following considerations. Firstly, as has been mentioned before, the equilibrium phase boundary has not been well constrained from the study of Yagi and Akimoto (1976). Secondly, systematic errors in pressure and temperature

determination are possibly introduced in comparing two studies because of different experimental techniques. It is therefore not straight-forward to compare the results of *in-situ* X-ray studies of Yagi and Akimoto (1976) and ours with those of Serghiou et al. (1995).

There is also recent speculation that thermal pressure may play an important role in the diamond-anvil cell (DAC) experiments conducted with a laser heating system and with argon as a pressure medium. Using a DAC technique that is basically identical to the one of Serghiou et al. (1995), Fiquet et al. (1995) have shown from an X-ray diffraction study that the measured volumes for MgO at high pressure and temperature are systematically smaller, by as much as 10%, than the values predicted by the quasi-harmonic equation of state. The possibility that these volume differences are due to systematic errors in temperature or to strong anharmonic behavior has been ruled out by Fiquet et al. (1995); they have consequently concluded that the determination of pressure is the major source of errors, due to the thermal pressure that increases significantly at the laser-heated spot. If this speculation is confirmed, it would certainly help to reconcile our experimental results with those of Serghiou et al. (1995), as can be seen in the insert of Fig. 11.

It is also very difficult to reconcile the experimental data of Serghiou et al. (1995) with the thermodynamic calculations of the slope dP/dT from the new calorimetric data of Akaogi et al. (1995) and Liu et al. (1996).

Acknowledgements We appreciate the helpful discussions and comments of M. Akaogi, F. Guyot, D.J. Weidner, T. Yagi and the two anonymous reviewers and the editor (I. Jackson). We also appreciate the assistance from M. Vaughan, Y. Wang, K. Kusaba, and J. Chen during the experiments. The Center for High Pressure Research (CHiPR) is jointly supported by the National Science Foundation (EAR 89-17563) and the State University of New York at Stony Brook. The *in situ* X-ray experiments were performed at the X-17B beamline of the National Synchrotron Light Source (NSLS) of the Brookhaven National Laboratory. The research is also supported by NSF grant EAR 93-04052. The MPI publication No. 142.

References

Akaogi M, Navrotsky A (1984) The quartz-coesite-stishovite transformations: new calorimetric measurements and calculation of phase diagrams. Phys Earth Planet Int 36: 124–134

Akaogi M, Yusa H, Shiraishi K, Suzuki T (1995) Thermodynamic properties of α quartz, coesite and stishovite and equilibrium phase relations at high pressures and high temperatures. J Geophys Res 100: 22337–22347

Akimoto S (1972) The system $MgO-FeO-SiO_2$ at high pressures and temperatures: phase equilibria and elastic properties. Tectonophys 13: 161–187

Akimoto S, Syono Y (1969) Coesite-stishovite transition. J Geophys Res 74: 1653–1659

Bohlen SR, Boettcher AL (1982) The quartz+coesite transformation: A precise determination and the effects of other components. J Geophys Res 87: 7073–7078

Cahn JW (1956) The kinetics of grain boundary nucleated reactions. Acta Metall 4: 313–320

Christian JW (1975) The theory of transformations in metals and alloys, Part I. Pergamon, New York

Decker DL (1971) High-pressure equation of state for NaCl, KCl, and CsCl. J Appl Phys 42: 3239–3244

Fei Y, Saxena SK, Navrotsky A (1990) Internally consistent data and equilibrium phase relations for compounds in the system $MgO-SiO_2$ at high pressure and high temperature. J Geophys Res 95: 6915–6928

Fiquet G, Andrault D, Itie JP, Gillet P, Richet P (1995) X-ray diffraction of periclase in a laser-heated diamond-anvil cell. Phys Earth Planet Interior (submitted)

Jackson I (1976) Melting of the silica isotypes SiO_2, BeF_2 and GeO_2 at elevated pressures. Phys Earth Planet Interior 13: 218–231

Kanzaki M (1991) Melting of silica up to 7 GPa. J Am Ceram Soc 73: 3706–3707

Liebermann RC, Wang Y (1992) Characterization of sample environment in a uniaxial split-sphere apparatus. In: Syono Y, Manghnani MH (ed) High-Pressure Research: Application to Earth and Planetary Sciences. AGU, Washington DC, pp 19–31

Liu J, Topor L, Zhang J, Navrotsky A, Liebermann RC (1996) Calorimetry study of the coesite-stishovite transformation and calculation of the phase boundary. Phys Chem Minerals 23: 11–16

Ostrovsky IA (1965) Experimental fixation of the position coesite-stishovite equilibrium curve. Izv Acad Sci USSR Geol Ser 10: 132–135

Saxena SK, Chartterjee N, Fei Y, Shen G (1993) Thermodynamic Data on Oxides and Silicates: an assessed data set based on thermochemistry and high pressure phase equilibrium. Springer-Verlag, Berlin, Heidelberg, New York

Serghiou G, Zerr A, Chudinovskikh L, Boehler R (1995) The coesite-stishovite transition in a laser-heated diamond cell. Geophys Res Lett 22: 441–444

Shen G, Lazor P (1995) Melting of minerals under lower mantle conditions: I. Experimental results. J Geophys Res 100: 17699–17713

Shimomura O, Utsumi W, Taniguchi T, Kikegawa T, Nagashima T (1992) A new high pressure and high temperature apparatus with sintered diamond anvils for synchrotron radiation use. In: Syono Y, Manghnani MH (ed) High-Pressure Research: Applications to Earth and Planetary Sciences. AGU, Washington DC, pp 3–11

Suito K (1977) Phase relations of pure Mg_2SiO_4 up to 200 kilobars. In: Manghnani MH, Akimoto S (ed) High Pressure Research: Application to Geophysics. Academic, San Diego, Calif, pp 365–371

Utsumi W, Weidner DJ, Liebermann RC (1994) Volume measurement of MgO under high pressures and high temperatures. EOS Trans AGU Fall Meeting Suppl 75: 696

Watanabe H (1982) Thermochemical properties of synthetic high-pressure compounds relevant to the Earth mantle. In: Akimoto S, Manghnani MH (ed) High-Pressure Research in Geophysics. Center for Academic Publications, Tokyo, pp 411–464

Weidner DJ, Vaughan MT, Ko J, Wang Y, Liu X, Yeganeh-haeri A, Pacalo RE, Zhao Y (1992) Characterization of stress, pressure, and temperature in SAM85, a DIA type high pressure apparatus. In: Syono Y, Manghnani MH (ed) High-Pressure Research: Application to Earth and Planetary Sciences. AGU, Washington DC, pp 13–117

Weidner DJ, Wang Y, Vaughan MT (1994) Yield strength at high pressure and temperature. Geophys Res Lett 21: 753–756

Yagi T, Akimoto S (1976) Direct determination of coesite-stishovite transition by *in situ* X-ray measurements. Tectonophysics 35: 259–270

Zhang J, Li B, Liebermann RC, Weidner DJ, Wang Y (1992) In situ X-ray study of the coesite-stishovite transition. EOS Trans AGU Fall Meeting 73: 566

Zhang J, Liebermann RC, Gasparik T, Herzberg CT, Fei Y (1993) Melting and subsolidus relations of SiO_2 at 9–14 GPa. J Geophys Res 98: 19785–19793

Zhang J, Li B, Utsumi W, Liebermann RC (1994) Reversal of the coesite-stishovite phase transformation. EOS AGU Spring Meeting 75: 346